EXPERIMENTAL CHARACTERIZATION OF THE FLOW OVER OPEN CAVITIES

Eduardo Augusto Florêncio Mega, eduardomega@dem.feis.unesp.br
Emileni Luzia Buainain Rosim, mi.rosim@yahoo.com.br
Edson Del Rio Vieira, delrio@dem.feis.unesp.br
Sérgio Said Mansur, mansur@dem.feis.unesp.br
UNESP Ilha Solteira, Av. Brasil Centro, 56, Ilha Solteira – SP, Brazil

Abstract. *In the present paper, flow inside open cavities has been experimentally investigated for different aspect ratios and Reynolds numbers up to* 10^4*. The tests have been conduced in a closed-loop free surface water channel. Topological structures of the flows have been identified with the help of two distinct visualizations techniques – liquid dye injection and solid micro-particles suspended in the water. Images have been captured by means of a still digital camera with several exposure times. Experimental results have shown that the use of solid tracers is particularly adequate for the visualization of stationary eddy structures. However, the use of that technique does not allow well identifying moving vortical structures such as Kelvin-Helmholtz instabilities usually formed in the shear region above the cavity. Velocity profiles have also been acquired in different stations by means of an acoustic Doppler velocimeter. The results obtained put in evidence some important physical characteristics of that class of flow and, at the same time, supply data for validating computational codes.*

Keywords*: Open cavity; Flow field; Flow visualization.*

1. INTRODUCTION

The flow past open cavities is frequently found in nature and technology. Vortex-shedding mechanism and eddy-wall characterizing that class of flow can produce severe ground erosion in valleys and depressions as well as noise, vibration, and premature failure in machines and equipments.

As a consequence of its practical importance, the fluid motion in cavities has been investigated by several authors for more than a half-century. Nevertheless most of the works in literature are devoted to compressible flows – such as Colonius *et al*. (1999a,b), Henderson *et al*. (2001), Ludovic *et al*. (2002), Gloerfelt *et al*. (2002), Gloerfelt *et al*. (2003a,b), Hamed *et al*. (2003), and Samimy *et al*. (2003) – and are concerned with controlling resonant instabilities and noise produced by aerodynamically induced pressure oscillations. The current available information concerning with incompressible flow is sharply smaller.

Shen and Floryan (1985) have numerically studied the incompressible flow in two-dimensional cavities with aspect ratio from 0.5 to 4 at very low Reynolds number, about 0.01. The results obtained by the authors have been confronted with available experimental data from the literature, presenting a good agreement.

Sinha *et al*. (1982) have experimentally investigated the flow within rectangular cavities with aspect ratio varying from 0.035 to 2.5, at three different values of Reynolds number – Re = 662, 1342, and 2648. That work has provided a useful database to validate numerical simulation codes and, for that reason, has become one of the main references about the subject for a long time.

Using laser Doppler velocimetry, Esteve *et al*. (2000) and Reulet *et al*. (2002) have studied the flow past a cavity with aspect ratio of 10, for Reynolds numbers 3.8 10^4 and 6.4 10^4. The flow field has been described in terms of velocity vectors and turbulence intensity, providing insight on the basic physics underlying the fluid dynamics behavior of large cavities at moderate Reynolds number.

In order to improve heat transfer process in solar collectors, Zdansky *et al*. (2000, 2001, 2003) have numerically simulated two-dimensional incompressible flows in open cavities. A wide range of Reynolds number has been considered by the investigators, including laminar and turbulent flows. In those latter computations a k-ε model has been employed for unsteady RANS closure.

Similar calculations have been carried out by Kim *et al.* (2001) in an investigation directed to pollutant dispersion in urban canyons. The unsteady flow past two buildings in side-by-side arrangement and a hill followed by two buildings downstream have been studied. The authors have shown that the flow patterns and the pollutant concentration depend strongly on the aspect ratio of the cavities.

The open cavity problem has been used by many authors for testing numerical modeling and computational fluid dynamics codes. In this context, Frigo (2004) has used such flow to evaluate an in-house CFD code. Similarly, Arruda (2004) has used the open cavity as a benchmark for testing the immersed boundary formulation proposed by Lima e Silva *et al*. (2003). In both cases, results obtained by the authors have been compared with experimental data of Sinha *et al*. (1982).

The present paper deals with the experimental investigation of water flow inside rectangular cavities with different aspect ratios b/h, where b is the cavity length and h its depth, as depicted in Fig.1. Flow visualizations have been performed at Reynolds numbers up to 10^4 using two classical techniques – liquid dye injection and solid micro-particles mixed in the work fluid. Additionally, flow velocity inside cavities has been measured by means of an acoustic Doppler velocimeter, providing reliable data for physical analysis and validation purposes.

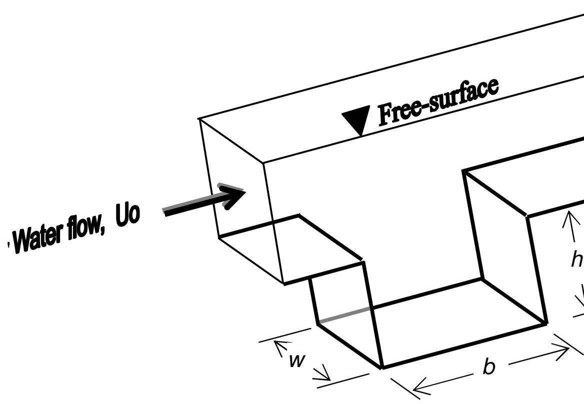

Figure 1: Open cavity geometric parameters.

2. EXPERIMENTAL APPARATUS AND PROCEDURE

Experimental runs have been performed in a free-surface water channel operating in closed-circuit. This apparatus consist of a centrifugal pump (*CP*), a flow control valve (*FC*), a diffuser (*DF*), a stabilization section (*SS*), a contraction (*CT*), a test section (*TS*), and a discharge reservoir (*DR*), disposed as indicated in Fig. 2(a). Honeycombs (*HC*) and screens (*SC*) are placed inside the stabilization section (*SS*) in order to damp disturbances upstream the contraction (*CT*) and to provide uniform stable flow in the test section (*TS*). The suction pipe (*SP*) has a diameter of 3" and is equipped with an electromagnetic flow meter (*FM*). The test section is built in transparent Plexiglas™ and has a rectangular transverse section with nominal size of 200 x 300 x 1200 mm. A long permanent cavity ($b/h = 10$) is positioned in its bottom surface, as depicted in Fig.2(b). An interchanging adapter has been constructed in order to allow simulating cavities with different aspect ratio. By replacing that adapter, three different cavities have been tested in this work, with $b/h = 0.5$, 1, and 2. In all the cases the sizes w, h, and d showed in Fig.2(b) have been kept unchanged.

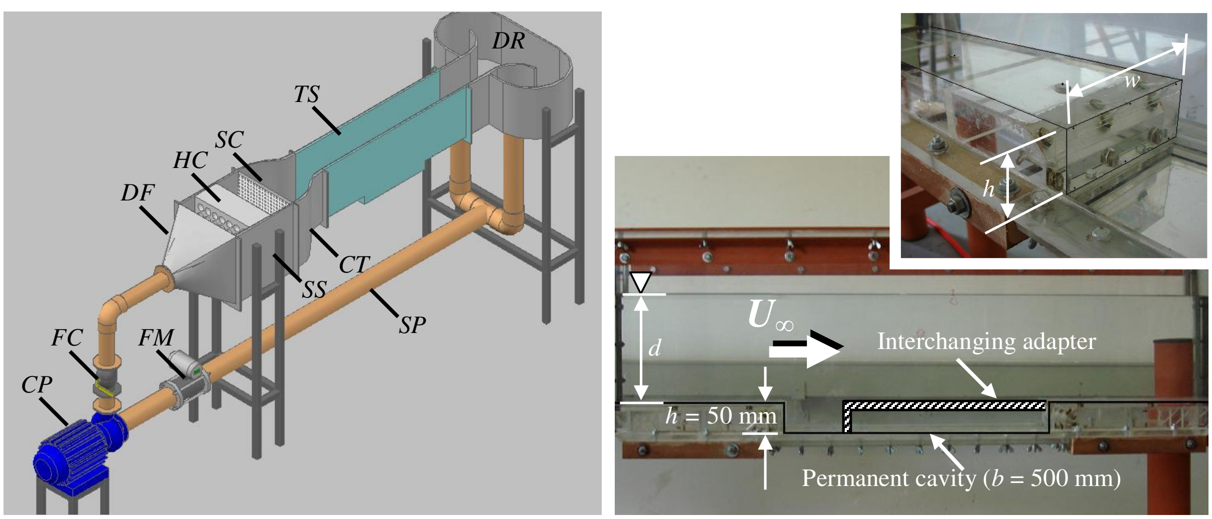

(a) Perspective view. (b) Test section details.

Figure 2: Closed-circuit free-surface water tunnel.

The maximum free-stream velocity in the test section is about 0.25 m/s, producing a Reynolds number (based on the depth h of the cavity and average uniform velocity U_o) about 10^4. Measurements performed with an acoustic Doppler velocimeter have put in evidence the satisfactory quality of the flow inside the test section, which combines adequate velocity profile and moderate turbulent intensity, mainly for highest velocities, when the turbulence level reach about 2%.

In the present tests, four Reynolds numbers based on the depth h have been adjusted, $Re = 10^3$, 2648, 5 10^3, and 10^4. The water flow rate has been determined with uncertainty of 1% using a previously calibrated electromagnetic flow meter.

Two classical flow visualization procedures have been used. Firstly, opaque liquid dye has been directly injected inside the cavity, with the help of an L-shape needle of 0.7 mm external diameter. Fluid flow images have been captured during dye wash process. A mix of PVA pigments, ethylic alcohol, and water, having viscosity and density nearly to the tap water, has been used as dye tracer. Diffuse back-light illumination has been necessary in order to produce sharp images with high contrast.

Secondly, solid micro-particles mixed in the flow have been used. In this case, a light-sheet system was employed to illuminate the region in the flow to be researched. When illuminated by a thin light-sheet, small particles suspended in the flow produce scattering of incident light and become sharply visible. In the image capture process, sufficiently long exposition times will result into streaks of the particles on the plane image. Obviously, in steady-state flows streamlines and pathlines can also be observed, since in that case they are coincident with streaklines.

Usually, light-sheet is produced by an expanding laser beam through a cylindrical lens or due to the projection of the beam on a rotating hexagonal mirror. In this work, the light-sheet was generated by the in-house system illustrated in Fig. 3, in which the laser source has been replaced by a Kodak™ carrousel slide projector. To prevent undesirable luminosity entrance in the test section, the runs have been carried out in the nocturnal period and all the experimental apparatus, including the still camera, was covered by a black canvas, as showed in Fig. 3(a). For obtaining the negative slide showed in Fig. 3(b), a white paper containing a single black straight line was photographed using black and white graphics negative film. So, the dark line on the white paper appears as a transparent line on the negative slide. When inserted in the slide projector, only that transparent line will allow light passing, generating a leaf illuminated in the flow.

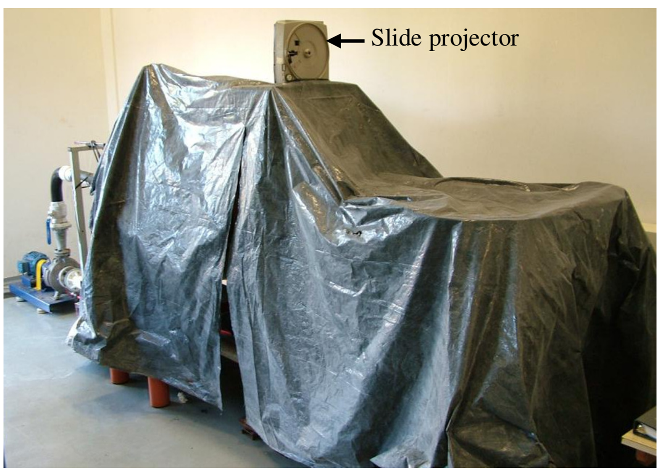

(a) Opaque black cover.

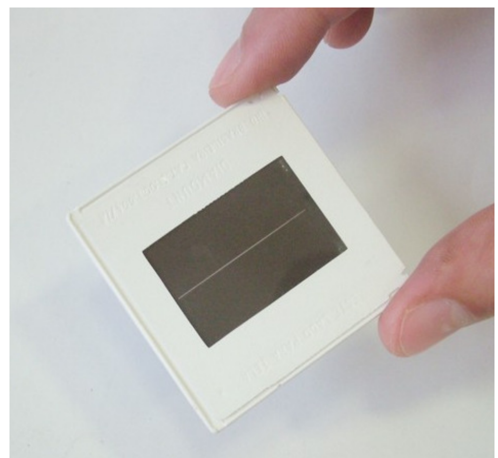

(b) High contrast negative slide.

Figure 3: Experimental apparatus covered by a black canvas and in-house light-sheet generator system for flow visualization.

Micro-particles of highly reflexive synthetic rubber have been used as solid tracers. Still photographs have been taken with a digital camera Fuji™ FinePix S7000 of 6.0 Megapixels and 6x optical zoom. Numerous preliminary tests have been performed in order to find the ideal exposition time to be adopted for each Reynolds number. To allow visual access to the flow and to facilitate framing and manual focalization operations, a high resolution monitor of 10" JVC™ CRT has been connected to the camera.

3. RESULTS AND DISCUSSION

Most of the time Reynolds number is sufficient to compare different flows. However, flow patterns inside cavities are also governed by the spatial scales that geometrically define the cavity, namely b and h, which can be combined to form another dimensionless parameter – the aspect ratio b/h. This double dependence makes a full reduction of the flow properties impracticable. As the aspect ratio is fixed, flow structure in cavities depends fundamentally on Reynolds number and vice-versa. So, the Reynolds number and the aspect ratio are both specified in each figure presented afterward.

Figure 4 presents flow patterns inside a cavity with $b/h = 1$ and different Re visualized with the help of solid micro-particles mixed into the water. The external flow direction is from left to right and the light sheet is fixed in the middle span of the cavity. Figure 5 shows images of the same flow obtained by liquid dye injection. It can be observed that sharper images are obtained using solid tracers, which allow accurately locating vortex kernels.

Figures 4(a) and 5(a) show that, for $Re = 10^3$, the separated shear layer rolls up into vortices and a single elongated eddy fills all the superior region of the cavity. The kernel of that vortical structure is situated near the right vertical wall, close to the cavity outlet, and the fluid in cavity bottom remains practically stagnant.

For more elevate Reynolds numbers, Fig. 4(b), (c), and (d) show that a large swirl having approximately the same cavity size is formed and the flow configuration became similar to that found in a lid-driven cavity. The kernel of these recirculations displaces toward the cavity center as *Re* increases from 2648 to 10^4. Two secondary eddies can be also identified in both inferior corners of the cavity, which improve their circulation as the Reynolds grows. According to Shen e Floryan (1985), these small eddies have been firstly identified and studied by Moffat (1964).

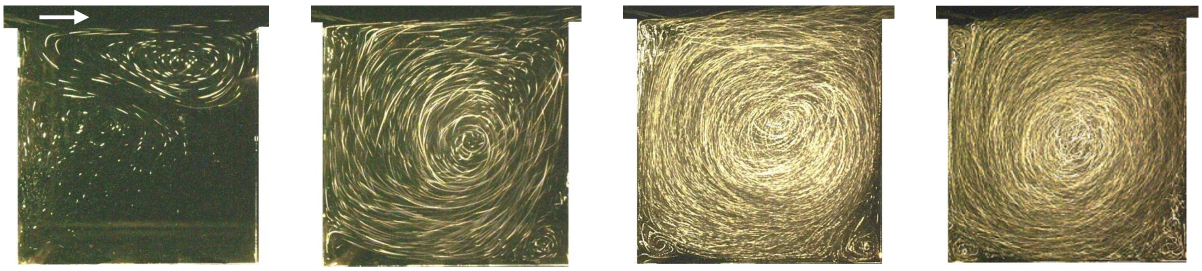

(a) $Re = 10^3$. (b) $Re = 2648$. (c) $Re = 5\ 10^3$. (d) $Re = 10^4$.

Figure 4: Flow visualization inside a cavity with $b/h = 1$ provided with the help of solid tracers.

(a) $Re = 10^3$. (b) $Re = 2648$. (c) $Re = 5\ 10^3$. (d) $Re = 10^4$.

Figure 5: Flow visualization inside a cavity with $b/h = 1$ provided with the help of liquid dye injection.

In this point, it is interesting to remark that distinct information can be extracted by using the two different visualization techniques employed. Indeed, for elevate Reynolds numbers, $Re = 5\ 10^3$ and 10^4, solid tracers in Fig. 4 show that the flow inside cavity is dominated by a large central vortex, while liquid dye injection in Fig. 5(c) and (d) makes evident the high diffusion that characterizes the process of transition to turbulence. Besides, Fig. 4(a) does not allow identify Kelvin-Helmholtz instabilities noticed in Fig. 5(a) at the horizontal shear zone that connects the flows inside and outside cavity.

Figure 6 presents the mean velocity profiles measured with the help of an ADV probe on the five stations represented in Fig. 6(f) at $Re = 2648$. The present results are compared with experimental data from Sinha *et al.*(1982) and numerical calculations by Arruda (2004). In all the cases a good agreement has been reached.

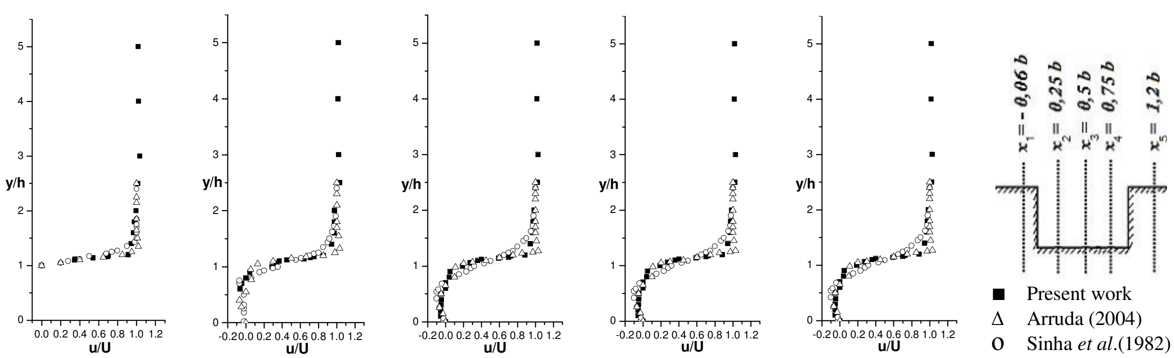

(a) $x_1 = -0.06\ b$ (b) $x_2 = 0.25\ b$ (c) $x_3 = 0.5\ b$ (d) $x_4 = 0.75\ b$ (e) $x_5 = 1.2\ b$ (f) Legend

Figure 6: Mean velocity profile (u) at different stations x, for $b/h = 1$ and $Re = 2648$.

Figure 7 presents images of the flow in an open cavity with aspect ratio $b/h = 0.5$, for different Reynolds numbers, obtained by using solid tracers. At $Re = 10^3$, Fig. 7(a), a still triangular vortex can be identified at the cavity top, as it has been early noticed in Fig. 4(a) and 5(a). For $Re = 2648$, this single vortex take on rounded shape with a characteristic size about h, but the fluid occupying the inferior portion of the cavity remains practically stationary.

As the Reynolds number reach higher values, Fig. 7(c) and (d), two vortical structures can be seen in the cavity, which are disposed one on the other. The upper structure turns in clockwise direction while the lower one rotates in the opposite direction.

In Fig. 8 the profiles of the mean velocity in the cavity centerline are presented for the different Reynolds numbers tested in this work. In the lower portion of the cavity no measurements have been performed due to the geometric characteristics of the ADV probe.

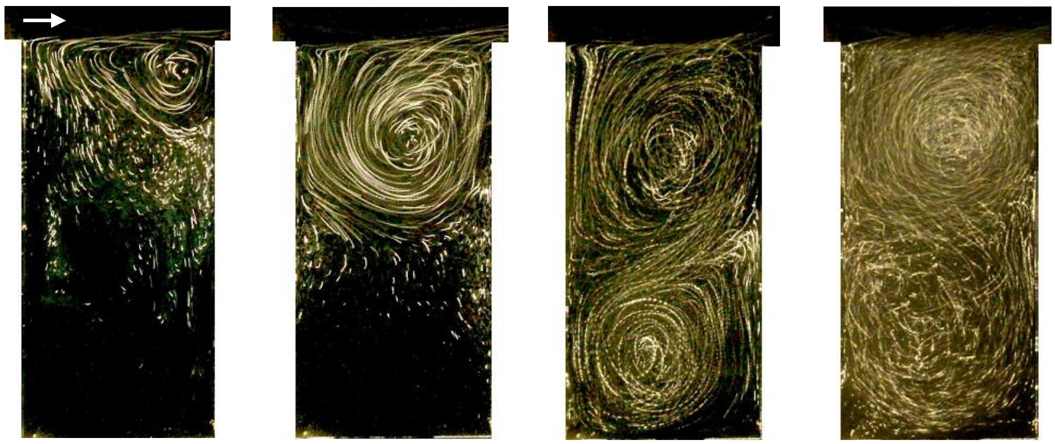

(a) $Re = 10^3$. (b) $Re = 2648$. (c) $Re = 5\ 10^3$. (d) $Re = 10^4$.

Figure 7: Flow visualization inside a cavity with $b/h = 0.5$ provided with the help of solid tracers.

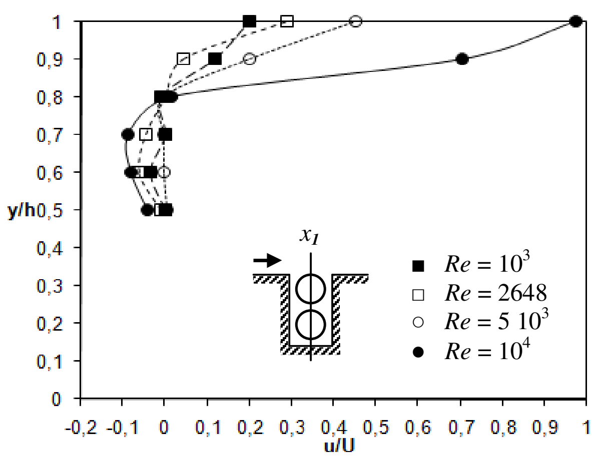

Figure 8: Mean velocity profile (u) at the cavity center line, for $b/h = 0.5$ and different Reynolds numbers.

Images in Fig. 9 and 10, obtained respectively by using solid tracers and liquid dye injection, show the flow in a cavity with $b/h = 2$, at different Reynolds numbers. At $Re = 10^3$, Fig. 9(a) and 10(a), the triangular vortex early identified remains at the superior boundary of the cavity. For more elevated Reynolds numbers – $Re = 2648$, $5\ 10^3$ and 10^4 – it can be perceived that the interaction between the internal flow and the free-stream in the canal above the cavity become more intense as compared with the precedent cases ($b/h = 1$ and 0.5). Physically, Kelvin-Helmholtz instabilities arise in the shear layer, as indicated in Fig. 10(c). These instabilities are advected downstream and collide with the right vertical wall of the cavity, producing periodic disturbances in the flow field inside the cavity. Genesis of the Kelvin-Helmholtz instabilities is well known and is associated with pronounced inflexional velocity profile that characterizes such a flow, which are presented in Fig. 11, where they are compared with numerical data from Arruda (2004).

For Re above $5\ 10^3$, the two contra-rotating swirls that appear vertically piled in Fig. 7(c) and (d) are replaced by two contra-rotating eddies with a characteristic size of b disposed side-by-side. So, the flow inside cavity is divided in two halves occupying the left and the right sides of the cavity. The rotational motion of the right vortex is sharply more intense than the left vortex. In Fig. 10(b), (c) and (d) only the right half flow appears recirculating.

(a) $Re = 10^3$.

(b) $Re = 2648$.

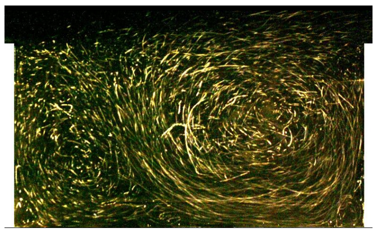

(c) $Re = 5\ 10^3$.

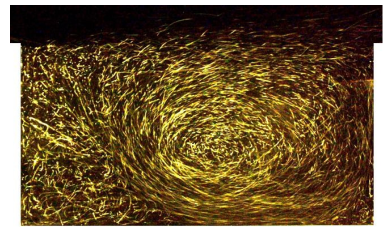

(d) $Re = 10^4$.

Figure 9: Flow visualization inside a cavity with $b/h = 2$ provided with the help of solid tracers.

(a) $Re = 10^3$.

(b) $Re = 2648$.

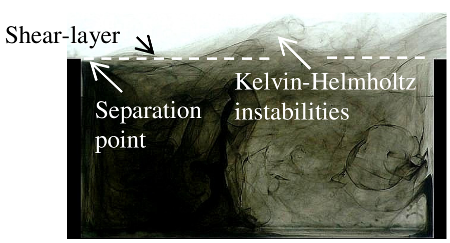

(c) $Re = 5\ 10^3$.

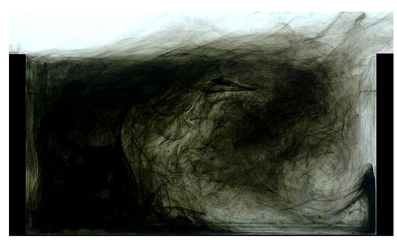

(d) $Re = 10^4$.

Figure 10: Flow visualization inside a cavity with $b/h = 2$ provided with the help of liquid dye injection.

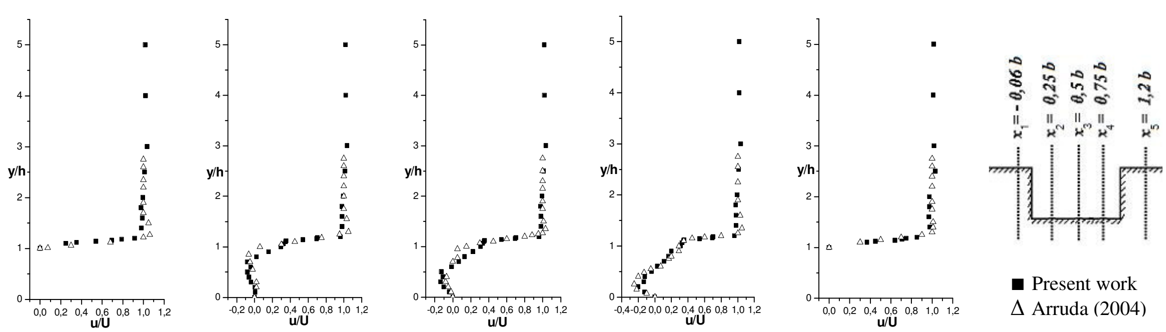

(a) $x_1 = -\,0.06\ b$ (b) $x_2 = 0.25\ b$ (c) $x_3 = 0.5\ b$ (d) $x_4 = 0.75\ b$ (e) $x_5 = 1.20\ b$ (f) Legend

Figure 6: Mean velocity profile (u) at different stations x, for $b/h = 2$ and $Re = 2648$.

4. CONCLUSION

In the present work, flow patterns inside open cavities have been qualitative and quantitatively investigated, for different aspect ratios and different Reynolds numbers. Two classical flow visualizations techniques have been employed in the experimental tests, i.e., liquid dye injection and solid tracers. Besides, measurements have been performed using an acoustic Doppler velocimeter, providing data for numerical modeling validations.

In spite the geometrical simplicity of that problem, cavity flows can became very complex, presenting stationary recirculation, shear-layer instabilities, periodic eddies, and other secondary vortical structures that continuously interact among themselves. The flow patterns depend strongly on the intensity of these interactions and can change considerably with aspect ratio and Reynolds number.

The two flow visualization techniques have been satisfactorily employed for providing different insights. In a general way, solid micro-particles suspended in the fluid flow illuminated by light sheet produce good-quality images, which allow sharply identifying stationary vortical structures. On the other hand, liquid dye injection is more appropriate to identify inherent moving instability of the shear layer past the cavity.

5. ACKNOWLEDGEMENTS

The authors are grateful to FAPESP, CNPq, and FUNDUNESP for the financial support given to this research. These acknowledgements are also extended to the Laboratório de Mecânica dos Fluidos Aplicada e Computacional – LAMAC, of the Universidade Federal do Rio Grande do Sul – UFGRS, which has kindly provided the solid micro-particles used in flow visualization experiments.

6. REFERENCES

Arruda, J.M., 2004, "Modelagem Matemática de Escoamentos Internos Forçados Utilizando o Método da Fronteira Imersa e o Modelo Físico Virtual", Ph.D. Thesis, Universidade Federal de Uberlândia – UFU, Uberlândia, Brazil.

Colonius, T., Basu, A.J., Rowley, C.W., 1999a, "Numerical Investigation of the Flow Past a Cavity", Proc. 5th AIAA/CEAS Aeroacustics Conference, Greater Seattle, Washington, USA.

Colonius, T., Basu, A.J., Rowley, C.W., 1999b, Computation of Sound Generation and Flow/Acoustic Instabilities in the Flow Past an Open Cavity, Proc. 3rd ASME/JSME Joint Fluids Engineering Conference, San Francisco, USA.

Esteve, M.J., Reulet, P., Millan, P., 2000, "Flow Field Characterization within a Rectangular Cavity", Proc. 10th International Symposium on Applications of Laser Techniques to Fluid Mechanics, Lisbon, Portugal.

Ludovic, B., Orkwis, P., Turner, M., 2002, "Modeling Unsteady Cavity Flows with Translating Walls", Proc. 32nd AIAA Fluid Dynamics Conference and Exhibit, St. Louis, USA.

Hamed, A., Basu, D., and Das, K., 2003, "Detached Eddy Simulations of Supersonic Flow over Cavity", Proc. 41st AIAA Aerospace Sciences Meeting and Exhibit, AIAA-2003-0549, Reno, USA.

Frigo, L.M., 2004, "Simulação Numérica de Escoamentos Incompressíveis Tridimensionais Turbulentos e em Transição", M.Sc. Dissertation, Universidade Estadual Paulista – UNESP, Ilha Solteira, Brazil.

Gloerfelt, X., Bailly, C., Juvé, D., 2002, "Simulation des Grandes Échelles du Champ Acoustique Produit par un Écoulement Affleurant une Cavité", Proc. 6ème Congrès Français d'Acoustique, pp.133-136, Lille, France.

Gloerfelt, X., Bailly, C., Juvé, D., 2003a, "Direct Computation of the Noise Radiated by a Subsonic Cavity Flow and Application of Integral Methods", Journal of Sound and Vibration, Vol.266, pp.119-146.

Gloerfelt, X., Bogey, C., Bailly, C., 2003b, "Numerical of Mode Switching in the Flow-Induced Oscillations by a Cavity", International Journal of Aeroacoustics, Vol.2, pp.99-124.

Henderson, J., Badcock, K.J., Richards, B.E., 2001, "Understanding Subsonic and Transonic Cavity Flows", The Aeronautical Journal, Vol.105, pp.77-84.

Kim, J.J., Baik, J.J., Chun, H.Y., 2001, "Two-Dimensional Numerical Modeling of Flow and Dispersion in the Presence of Hill and Buildings", Journal of Wind Engineering and Industrial Aerodynamics, Vol.89, pp.947-966.

Lima e Silva, A.L.F., Damasceno, J.J.R., Silveira-Neto, A, 2003, "Numerical Simulation of Two Dimensional Flows over a Circular Cylinder Using the Immersed Boundary Method", Journal of Computational Physics, Vol.189, pp.351-370.

Moffat, H.K., 1964, "Viscous and Resistive Eddies near a Sharp Corner", Journal of Fluid Mechanics, Vol.18, pp.1-18.

Reulet, P., Esteve, M.J., Millan, P., Riethmuller, M.L., 2002, "Experimental Characterization of the Flow within a Transitional Rectangular Cavity", Journal of Flow Visualization and Image Processing, Vol.9, pp.153-170.

Samimy, M., Debiasi, M., Caraballo, E., Özbay, H., Efe, M.Ö., Yuan, X., DeBonis, J., Myatt, J.H., 2003, "Development of Closed-Loop Control for Cavity Flows", Proc. 33rd AIAA Fluid Dynamics Conference and Exhibit, Orlando, USA.

Shen, C., Floryan, J.M, 1985, "Low Reynolds Number Flow over Cavities", Physics of Fluids, Vol.28, pp.3191-3202.

Zdanski, P.S.B., Ortega, M.A., Fico Jr., N.G.C.R., 2000, "Numerical Simulation of Laminar Flow over Shallow Cavities", Proc. 8th Brazilian Congress of Engineering and Thermal Sciences – ENCIT, Porto Alegre, Brazil.
Zdanski, P.S.B., Ortega, M.A., Fico Jr., N.G.C.R., 2001, "Numerical Simulation of Turbulent Flow over Shallow Cavities", Proc. 2nd International Conference on Computational Heat and Mass Transfer, Rio de Janeiro, Brazil.
Zdanski, P.S.B., Ortega, M.A., Fico Jr., N.G.C.R., 2003, "Numerical Study of the Flow over Shallow Cavities", Computers & Fluids, Vol.32, pp.953-974.

7. RESPONSIBILITY NOTICE

The authors are the only responsible for the printed material included in this paper.